

Extinction in Deformed Copper Single Crystals. A Combined Study by γ -ray Diffractometry and Neutron Structure Refinement

BY MOGENS S. LEHMANN

Institut Max von Laue–Paul Langevin, BP 156X Centre de Tri, F-38042 Grenoble CEDEX, France

AND JOCHEN R. SCHNEIDER*

Hahn-Meitner-Institut, Glienicker Strasse 100, D-1000 Berlin 39, Federal Republic of Germany

(Received 8 December 1976; accepted 16 March 1977)

Neutron diffraction and γ -ray rocking-curve measurements were performed on plastically deformed single crystals of Cu in order to compare the mosaic distribution parameters obtained from least-squares structural refinement with those seen by the γ -diffractometer. Neutron data were collected at two wavelengths ($\lambda = 0.538$ and 0.741 Å) for one crystal with very homogeneous mosaic distribution, and for another crystal with less good but more typical mosaic structure data were collected for $\lambda = 0.538$ Å. Maximum $\sin \theta/\lambda$ was 1.52 Å⁻¹ and maximum extinction correction was less than 30%. For the latter crystal no comparison could be made between the two sets of observed distribution parameters because of the uneven mosaic distribution. The former crystal was found from the γ -ray measurements to be bent, but when this was taken into consideration in the Coppens–Hamilton [*Acta Cryst.* (1970), A26, 71–83] formalism for anisotropic extinction correction good agreement was found between mosaic parameters obtained by γ -ray and neutron measurements for directions not affected by the crystal curvature, whereas the structure refinement did not, as expected, reflect the complete crystal curvature when this effect was dominant.

Introduction

It is at present possible to correct in a routine manner for the effect of secondary extinction in X-ray and neutron diffraction measurements on imperfect single crystals, *i.e.* samples showing an integrated reflecting power R_{meas} somewhere in between the theoretical values obtained from the kinematical and the dynamical theories of diffraction. Theories are available (Zachariasen, 1967; Becker & Coppens, 1974) which within the framework of intensity coupling describe the relationships between the reduction in the observed intensities with respect to the value expected from the kinematical theory and the defect arrangement in the crystal. If the parameters which describe the defect structure in the sample are known, then in principle the correction for extinction is straightforward. In practice, however, it is difficult to determine these parameters either because measurement techniques are not available or because it is impossible to describe the defect arrangement in the simple analytical form to which the theory applies. Least-squares refinement programs have therefore been set up (Larson, 1969; Coppens & Hamilton, 1970) which include extinction parameters as variables in the structure-refinement process. In general this approach leads to a much improved agreement between observed and calculated structure amplitudes even in cases where the extinction corrections are a major part of the calculated quantity. We are then however un-

fortunately left with parameters for the description of the crystal defect structure which either we cannot check using independent measurements or we suspect are physically meaningless. Thus in order to estimate the validity of the theory as well as to compare various theories we must in most cases have recourse to comparisons among agreement factors between observed and calculated quantities or to a study of the values of other parameters in the refinement, such as thermal motion parameters, which are found to be sensitive to the extinction correction.

Recently Bonnet, Delapalme, Becker & Fuess (1976) applied the Becker & Coppens theory to the polarized neutron technique and found the correction to be quite adequate even for reflexions strongly affected by extinction. The authors stress that investigations of the behaviour of the flipping ratio are well suited to study the effect of the assumed angular distribution of the mean diffracting power $\bar{\sigma}$ because they are free of any scaling problem. Cooper & Rouse (1976) compared the extinction theory of Becker & Coppens (1974*a,b*; 1975) with their own theory (Cooper & Rouse, 1970). For the comparison they used agreement factors and temperature parameters as well as the domain radius r and the mosaic spread parameter g obtained with the two theories from data sets measured for two samples with X-rays and neutrons at a series of different wavelengths. The authors conclude that provided r is much smaller than the mean pathlength \bar{T} of the radiation in the crystal both extinction formalisms give good agreement for data at any one wavelength, but that neither of the formalisms

* Work supported by Deutsche Forschungsgemeinschaft.

accounts correctly for the wavelength dependence of the secondary extinction.

In this paper we do not intend to contribute to the discussion on which theory is a better approximation, but we do want to emphasize that all extinction theories used in crystal structure refinements describe the defect structure of the sample essentially on the basis of Darwin's (1914, 1922) mosaic model, which in general is only a crude approximation to the real defect structure in imperfect single crystals. We feel strongly that all discussion of the reliability of these extinction theories is incomplete if it is not checked experimentally that the defect structure of the investigated sample can be described by a mosaic model. Cooper & Rouse (1976) note that for the investigation of extinction neutron diffraction studies have a number of advantages. Firstly, the neutron scattering lengths are essentially independent of angle so that significant extinction effects are not restricted to small Bragg angles. Additionally, the absorption of neutrons in the sample and the effects of primary extinction are usually small. However, the samples are rather large and it is not evident that the defect structure in these crystals can be described on the basis of Darwin's mosaic model (see, for example, Schneider, 1976, 1977). If the mosaic structure has inhomogeneities, especially of the type *B* (Schneider, 1975*a*), the domain radius *r* and the mosaic spread parameter *g* as determined from structure refinements have no physical meaning. Therefore one may question whether these two parameters are suitable for a discussion of the reliability of two different extinction theories, if it is not checked that the crystal defects are statistically distributed within the sample.

Mosaic distribution functions $W(\omega)$ can be determined directly from rocking curves measured by means of γ -ray diffractometry (Schneider, 1974*a, b*), if the fine structure in $W(\omega)$ is large compared to the horizontal divergence of the incident γ -ray beam ($\sim 10''$). In a typical experiment the wavelength of the γ -radiation is 0.03 Å making the absorption and extinction effects negligible. It is therefore possible – at least for a few simple compounds – to carry out measurements in which a direct comparison can be made between mosaic distributions obtained from γ -ray rocking curves and the corresponding extinction parameters obtained from structure refinements. In order to make such a comparison we designed the following experiment: A copper single crystal was chosen as specimen, as this material can be plastically deformed to obtain a well-defined mosaic distribution (Seeger, 1965). The dimensions of the sample were chosen in a range suitable for both γ -ray and neutron diffraction measurements. The samples were rather strongly deformed so that firstly the mosaic spread parameter could be expected to dominate the influence of the particle size parameter, and secondly so that the extinction effect is not bigger than about 30%, whereby the difference between the different

theories of secondary extinction can be assumed to be rather small.

γ -ray measurements

The γ -ray instrument is a single-crystal diffractometer employing radiation with an energy of 412 keV ($\lambda = 0.0302$ Å, $\Delta\lambda/\lambda = 10^{-6}$) from a radioactive gold source. The beam is collimated into a cross section of 0.2×10 mm, corresponding to a horizontal divergence of $\sim 10''$ and a vertical divergence of $\sim 8'$. Because of the small Bragg angles the samples are studied in Laue geometry and only lattice tilts contribute to the half-width of the rocking curve (Freund & Schneider, 1972). The wavelength is sufficiently small for possible deformations of the rocking curves due to multiple Bragg scattering to be avoided (Schneider, 1975*b*).

Large nearly perfect copper single crystals were deformed plastically by A. Freund (1975*b*) in order to produce good neutron monochromators. A cube of 16 mm^3 was carefully cut out of one of these crystals by spark erosion and etched to the final dimensions shown in Fig. 1. Rocking curves around ω were measured for the reflexions 111, $2\bar{2}0$ and $22\bar{4}$ for a series of azimuthal angles ψ (as defined in Fig. 1), and from this the integrated reflecting power was derived. As the values found were always very close to the kinematical value, the mosaic distribution $W(\omega_v)$ is obtained directly from the Bragg scattered intensity as

$$W(\omega_v) = \frac{P_H(\omega_v) - B}{\sum_{v=1}^N (P_H(\omega_v) - B) \Delta\omega},$$

where *B* represents the background, *N* is the number of steps in the rocking curve and $\Delta\omega = \omega_{v+1} - \omega_v$ is the step width in the ω scan. Figs. 2 to 4, which show mosaic distributions derived from the rocking curves

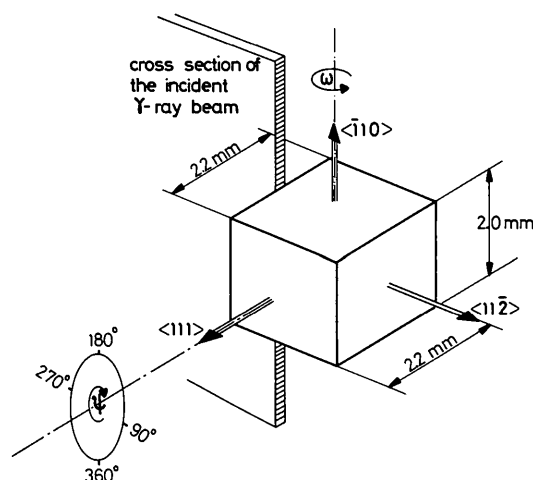


Fig. 1. Dimensions and orientation of the small copper crystal with respect to the cross section and direction of the incident beam of the γ -diffractometer. ω is the rocking angle and ψ is the angle describing the rotation of the sample around the scattering vector.

for different azimuthal angles ψ for the reflexions 111, 220 and 224, indicate that the mosaic structure of the sample is rather homogeneous but extremely anisotropic, the mosaic spread varying from about 5 to 30'.

We have to emphasize though that this copper crystal shows an unusually homogeneous mosaic structure. Another slightly larger crystal of dimensions $3.5 \times 3.5 \times 3.5$ mm cut in a similar fashion to the crystal discussed above was studied for comparison, and it showed a much less uniform mosaic distribution. In Fig. 5 a series of mosaic distributions $W(\omega)$ is plotted which was obtained from γ -ray rocking curves for the 111 reflexion measured in a series of volume elements. From γ -ray measurements in a great number of crys-

tals we have found that this type of mosaic structure is representative of the majority of imperfect single crystals used in neutron diffraction experiments.

Neutron diffraction measurements and structure refinement

Neutron diffraction data were collected at room temperature on the four-circle diffractometer *D9* located at the hot source of the Institut Laue-Langevin high flux beam reactor. Pertinent data are summarized in Table 1. Measurements were carried out on the two crystals described above using wavelengths of 0.538 and 0.741 Å for the small crystal and a wavelength of

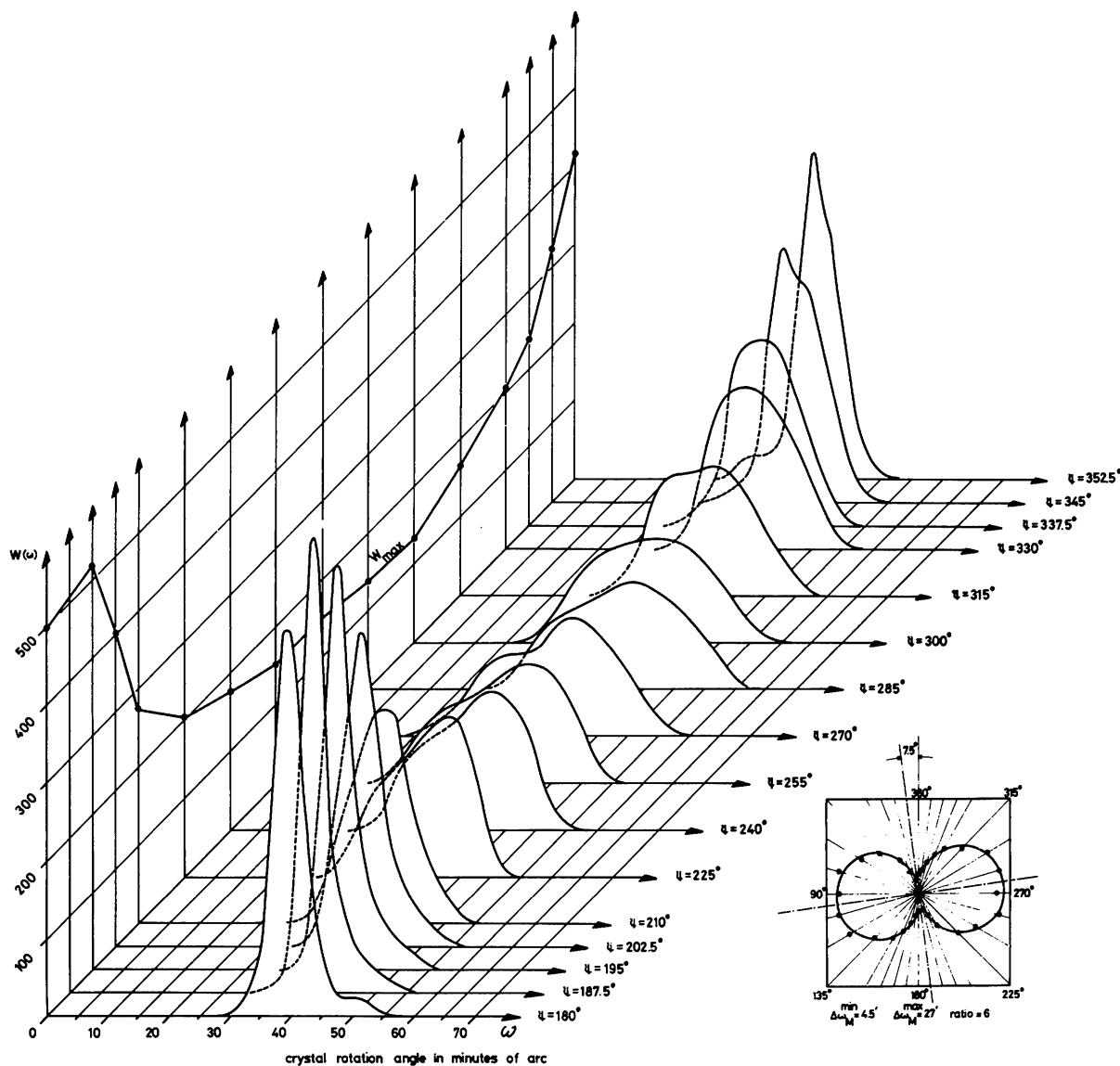


Fig. 2. Mosaic distributions $W(\omega)$ deduced from γ -ray rocking curves measured in the small crystal at the 111 reflexion for different azimuthal angles ψ . Cross section of the incident γ -ray beam 0.5×10 mm, horizontal divergence $\sim 30'$. The eight-shaped curve represents a plot in polar coordinates of the FWHH $= \Delta\omega_M$ of $W(\omega)$ as a function of ψ .

0.538 Å for the large crystal. The monochromatic neutron beam was obtained by reflexion from the (200) plane of a Cu crystal in transmission geometry. Coupled ω - 2θ step scans were used to record the reflexion profiles in the bisecting geometry, and the number of steps for each profile was 48. The steplength was varied as a function of the Bragg angle so that approximately half the points were recordings of background. The crystals were mounted with the [111] direction near, but not parallel to the ϕ axis of the diffractometer, and all reflexions with $h, k, l \geq 0$ were measured. The stability of the recording equipment was monitored by measurement of two standard reflexions

(111 and 400) at intervals of 25 reflexions, but no non-statistical variation was observed. As a part of the measurements rocking curves were made for the 222 reflexion for a series of ψ angles similar to the γ -ray measurements. The results are discussed below and are represented in Fig. 7.

Profiles were reduced to F^2 values with the minimal $\sigma(I)/I$ criteria (Lehmann & Larsen, 1974), where I is the integrated intensity and $\sigma(I)$ its standard deviation. Absorption corrections were applied by the Gaussian numerical integration method followed by correction for second-order contamination. Both of these corrections were very small and gave in all cases rel-

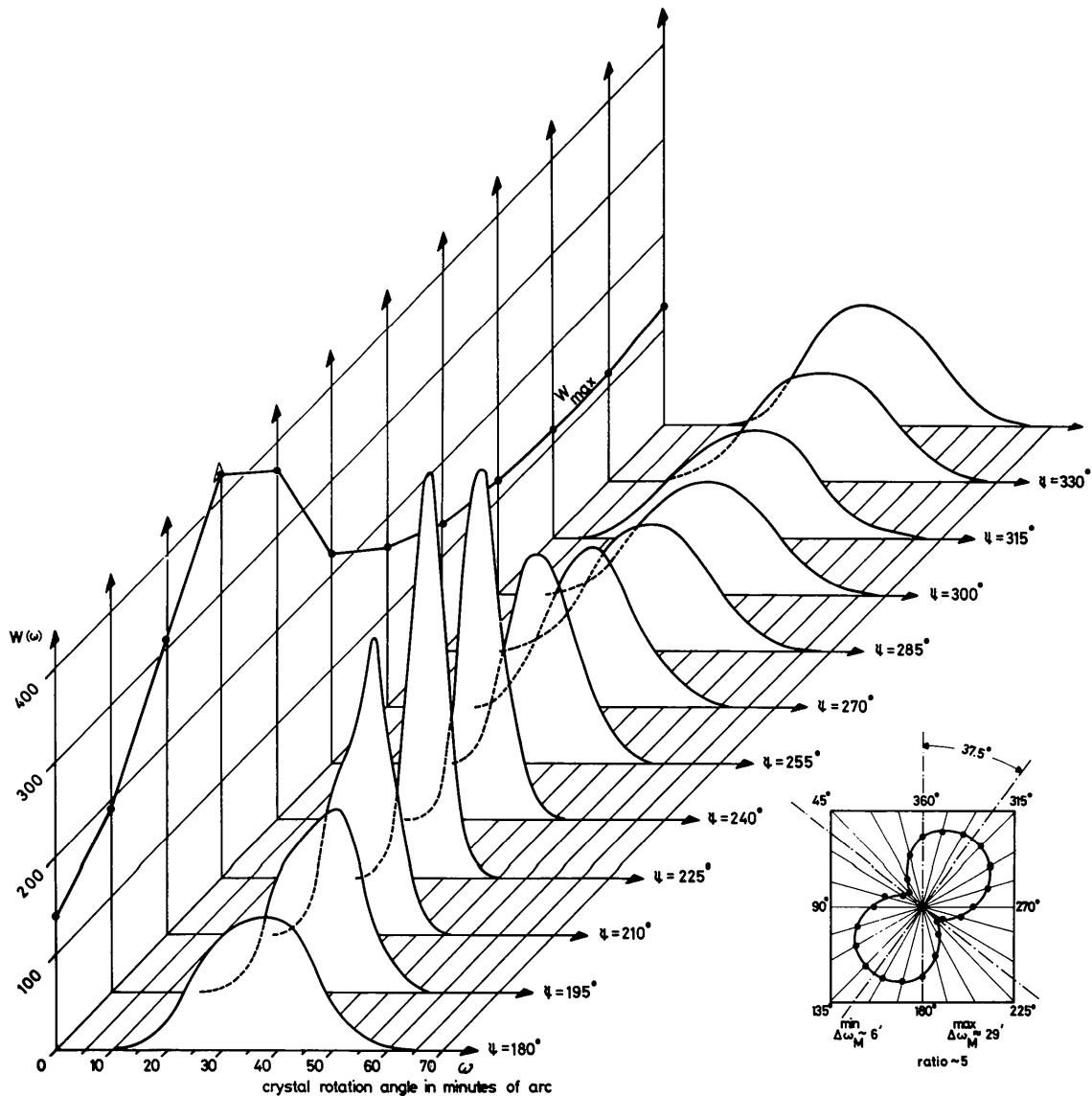


Fig. 3. Mosaic distributions $W(\omega)$ deduced from γ -ray rocking curves measured in the small crystal at the $2\bar{2}0$ reflexion for different azimuthal angles ψ . Cross section of the incident γ -ray beam 0.5×10 mm, horizontal divergence $\sim 30'$. The eight-shaped curve represents a plot in polar coordinates of the $\text{FWHH} = \Delta\omega_M$ of $W(\omega)$ as a function of ψ .

Table 1. Summary of common crystal and experimental parameters for the neutron measurements

Cu single crystals $a = 3.61496 \text{ \AA}$		
Space group $Fm\bar{3}m$		
Scattering length $0.76 \times 10^{-12} \text{ cm}$		
Wavelengths λ (\AA)	0.538	0.741
Maximum $\sin \theta/\lambda$ (\AA^{-1})	1.52	1.14
Number of reflexions N	256	100
Absorption factor* μ , (cm^{-1})	0.09	0.13
Second-order contamination (%)	0.45†	0.85‡

* From *Neutron Cross Sections* (1955).

† Estimated.

‡ Observed.

ative changes in F^2 of less than 1%. The data were corrected neither for thermal diffuse scattering nor for contributions from multiple Bragg scattering.

Least-squares refinements were carried out using the *LINEX* program of the Buffalo computing system (Coppens, 1975), which includes options for refinement of extinction parameters following the theory of Becker & Coppens (1974, 1975). Quantities relevant for the refinement as well as the refined parameters are given in Table 2. The quantity minimized was $S = \sum W(F_o^2 - k^2 F_c^2)^2$ with $W = 1/[\sigma^2(\text{counting}) + (pF_o^2)^2]$, where the summation is over all sets of observed and calculated structure factors F_o , F_c and

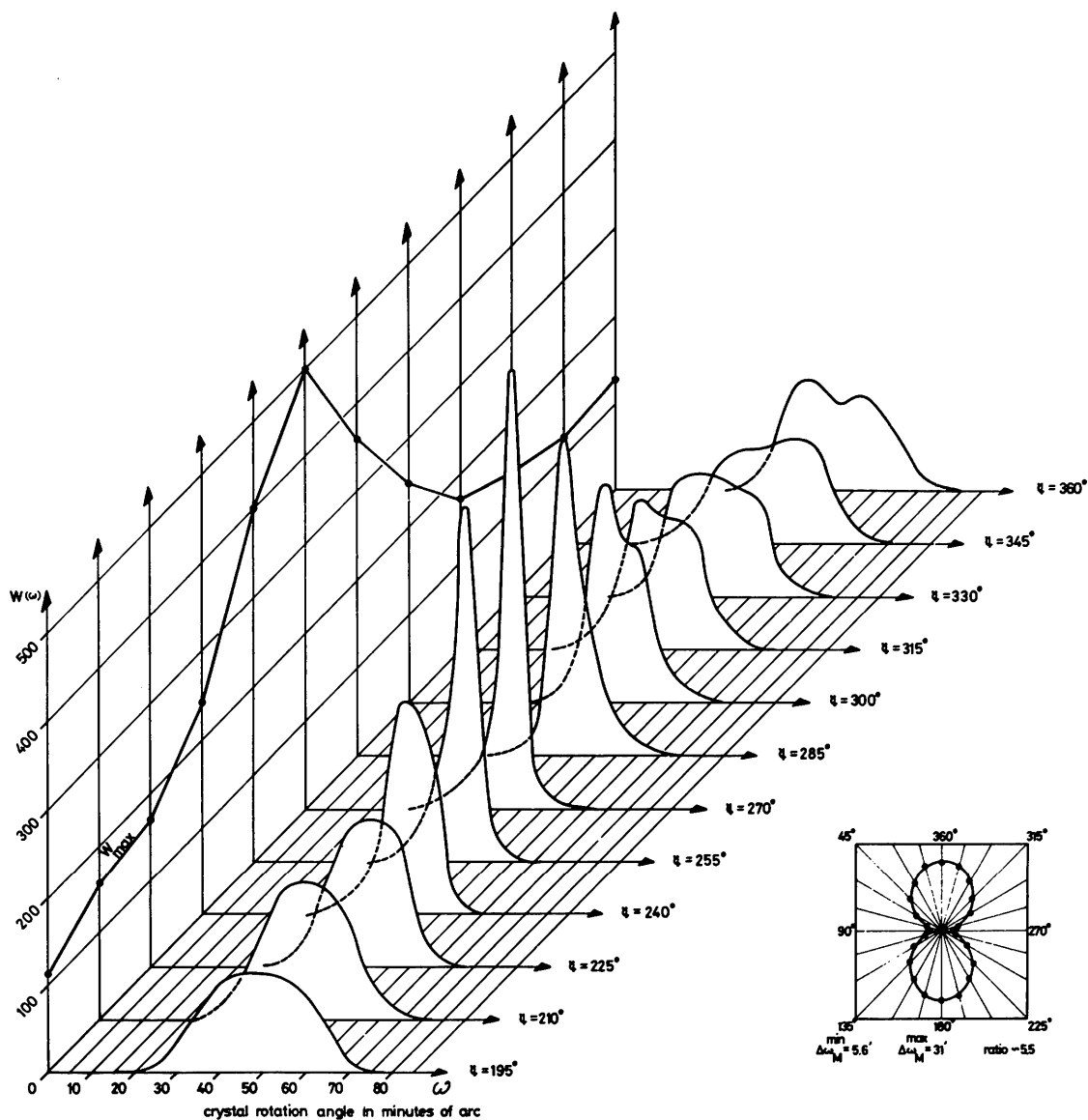


Fig. 4. Mosaic distributions $W(\omega)$ deduced from γ -ray rocking curves measured in the small crystal at the $22\bar{4}$ reflexion for different azimuthal angles ψ . Cross section of the incident γ -ray beam $0.5 \times 10 \text{ mm}$, horizontal divergence $\sim 30'$. The eight-shaped curve represents a plot in polar coordinates of the $\text{FWHM} = \Delta\omega_M$ of $W(\omega)$ as a function of ψ .

where p in the weight equation was varied in order to approximate the goodness-of-fit, $[S/(N-b)]^{1/2}$, to a value of one, with N and b the number of observations and the number of variables respectively.

The extinction was, as discussed above, treated according to the type I approximation, *i.e.* mainly determined by the mosaic spread in the crystal, and with the guidance of γ -ray rocking curves a Gaussian description of the mosaic distribution was used. Refinements assuming isotropic extinction for both crystals and anisotropic extinction for the large crystal posed no problem and the results are given in Table 2, but for the small crystal the tensor describing the anisotropic mosaic distribution was non-positive definite preventing convergence in this refinement. Following Coppens & Hamilton (1970) the mosaic spread parameter $\eta(\mathbf{D})$ in the scattering plane orthogonal to \mathbf{D} (a unit vector in the crystal axis system) is given by

$$\eta(\mathbf{D}) = \frac{1}{2\pi^{1/2}} \cdot \frac{1}{g(\mathbf{D})} = \frac{1}{2\pi^{1/2}} \cdot \frac{1}{(\mathbf{D}'\mathbf{Z}\mathbf{D})^{1/2}} \quad (1)$$

where Z is the extinction tensor. By means of Z an ellipsoid can be constructed which describes the anisotropic mosaic distribution. The curves plotted in Figs. 2 to 4 giving the mosaic parameter as a function of the rotation angle ψ around the scattering vector for a given reflexion are sections through the centre of this ellipsoid, so in the frame of the Coppens & Hamilton theory the ellipsoidal description of the anisotropic distribution is not adequate for this sample. To improve the description an additional parameter η^* was introduced in (1):

$$\eta(\mathbf{D}) = \sqrt{\frac{1}{4\pi\mathbf{D}'\mathbf{Z}\mathbf{D}} - (\eta^*)^2}, \quad (2)$$

giving a peanut-shell shaped surface. The extinction

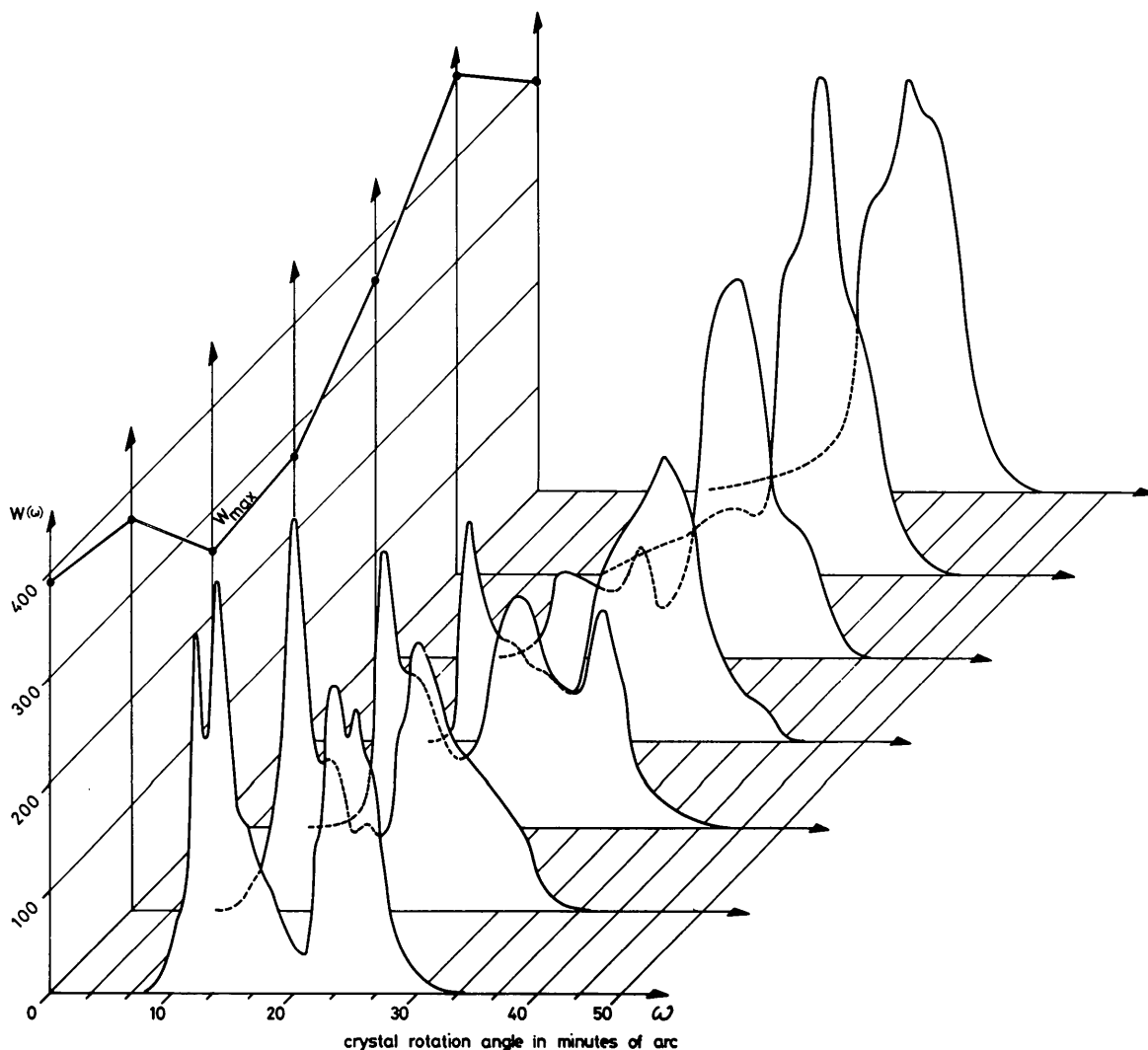


Fig. 5. Mosaic distributions $W(\omega)$ deduced from γ -ray rocking curves measured in a series of sections through the large crystal. Reflexion 111. Cross section of the incident γ -ray beam 0.2×10 mm, horizontal divergence $\sim 10'$. Distance between neighbouring sections 0.5 mm.

Table 2. Final parameters from the neutron refinements

p , the weight factor, and g.o.f., the goodness-of-fit, are defined in the text. The models are: *I*, isotropic, *AP*, anisotropic peanut-shell shape, *AE*, anisotropic ellipsoidal shape for the mosaic distribution. The R values are

$$\begin{aligned} R_F &= \Sigma |F_o - F_c| / \Sigma F_o \\ R_{WF} &= (\Sigma W |F_o - F_c|^2 / \Sigma W F_o^2)^{1/2} \\ R_{F^2} &= (\Sigma |F_o^2 - F_c^2| / \Sigma F_o^2)^{1/2} \\ R_{WF^2} &= (\Sigma W |F_o^2 - F_c^2|^2 / \Sigma W F_o^4)^{1/2}. \end{aligned}$$

The scale factor is arbitrarily set to 1.000 for the anisotropic refinements. The temperature factor is defined from the structure-factor equation as $F = 4b_{Cu} \exp[-8\pi^2 u(\sin \theta/\lambda^2)]$ where b_{Cu} is the scattering length for Cu. The lowest E is the largest extinction correction in the set.

Standard deviations in this table and throughout the paper are given in parenthesis in unit of the last digit.

Crystal	Small				Large	
$\lambda(\text{\AA})$	0.538	0.538	0.741	0.741	0.538	0.538
$p(\%)$	1.2	1.2	1.5	1.5	3.0	3.0
Model	<i>I</i>	<i>AP</i>	<i>I</i>	<i>AP</i>	<i>I</i>	<i>AE</i>
g.o.f.	1.26	1.04	2.36	0.98	1.47	1.40
$R_F(\%)$	0.9	0.8	1.3	0.6	1.7	1.7
$R_{WF}(\%)$	1.3	1.0	1.3	0.6	1.7	1.7
$R_{F^2}(\%)$	1.8	1.5	2.8	1.2	3.4	3.3
$R_{WF^2}(\%)$	2.5	2.1	2.5	1.1	3.5	3.3
Scale	1.009 (3)	1.000 (3)	1.070 (6)	1.000 (5)	1.008 (5)	1.000 (7)
$u(\text{\AA}^2)$	0.00633 (3)	0.00627 (2)	0.00708 (8)	0.00648 (5)	0.00654 (4)	0.00648 (5)
$g \times 10^{-1}$	40 (3)		74 (3)		53 (2)	
$Z_{11} \times 10^{-3}$		16 (2)		17 (1)		49 (13)
$Z_{22} \times 10^{-3}$		17 (2)		17 (1)		15 (4)
$Z_{33} \times 10^{-3}$		18 (2)		20 (1)		34 (9)
$Z_{12} \times 10^{-3}$		-5 (1)		-5 (1)		-5 (5)
$Z_{13} \times 10^{-3}$		0 (1)		0 (1)		-16 (7)
$Z_{23} \times 10^{-3}$		-1 (1)		0 (1)		-7 (2)
$\eta^*(\prime)$		380		380		
Lowest E	0.86	0.81	0.64	0.67	0.69	0.70

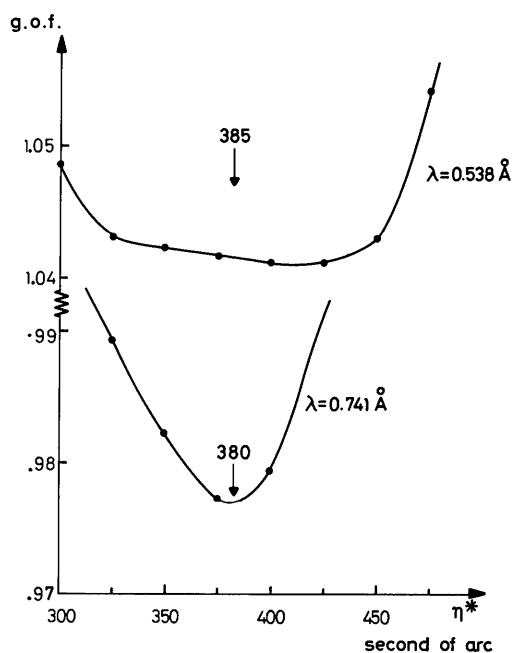


Fig. 6. Goodness-of-fit (g.o.f.) from the refinements of the data from the small crystal as a function of the parameter η^* defined in (2).

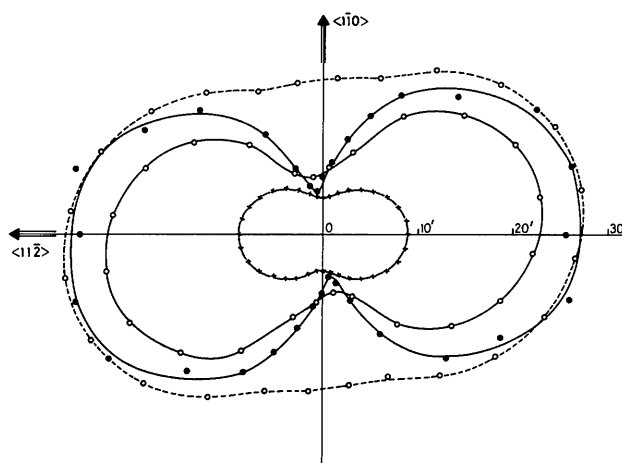


Fig. 7. Mosaic spread for the small crystal as a function of rotation around the scattering vector 111: \times - \times - \times cut through the mosaic distribution deduced from the crystal structure refinement, \bullet - \bullet - \bullet result obtained by γ -ray diffractometry, \circ - \circ - \circ FWHH of the measured neutron profile, \circ - \circ - \circ FWHH of the neutron profiles after a Gaussian deconvolution of the measured profiles with the resolution function of the neutron diffractometer, which in agreement with direct measurements was estimated to have a FWHH of $\sim 16'$. The average standard deviation for the values derived from refinement results is $1'$.

parameter $g'(\mathbf{D})$ for a scattering plane orthogonal to \mathbf{D} is then given as

$$g'(\mathbf{D}) = \sqrt{\frac{\mathbf{D}'\mathbf{Z}\mathbf{D}}{1 - 4\pi\mathbf{D}'\mathbf{Z}\mathbf{D}(\eta^*)^2}}$$

This expression was incorporated in the least-squares refinement, and refinements of the \mathbf{Z} tensor were carried out for a series of η^* values. The goodness-of-fit was used to indicate the quality of the agreement, and Fig. 6 shows this quantity as a function of η^* . Choosing the midpoint of the very shallow minimum for the short-wavelength curve and the minimum point for the long-wavelength curve good agreement is obtained between η^* and Z_{ij} for the two wavelengths, but even a choice of η^* equal to $425''$ corresponding to the minimum goodness-of-fit for the short-wavelength data does not influence the mosaic distribution parameters as represented in Fig. 7 by more than at maximum $2'$. The results of the final refinement with $\eta^* = 380''$ are given in Table 2, and the observed and calculated structure amplitude for the three final anisotropic refinements are given in Table 3.†

In order to test the stability of the refined parameters with respect to variations in the weighting scheme additional refinements were carried out on the data for the small crystal with $W = 1/\sigma^2$ (counting) and $W = 1$, and all changes were found to be less than one standard deviation. Likewise low and high-order refinements were carried out, where the low- and high-order halves of the data were refined independently. This time changes in the temperature parameter were slightly higher with an increase for the low-order data. However, for both wavelengths the change was less than two standard deviations, *i.e.* less than 2% of the observed value.

Discussion

Table 2 summarizes the parameters obtained from the three sets of neutron data. Before a comparison is made with the results from the γ -ray measurements it is worth while discussing some features of these refinements.

First we note that the various R values are smaller for the small crystal, despite the fact that from a counting-statistical point of view the structure amplitudes for the two crystals were determined with approximately the same precision. As the extinction corrections are only slightly bigger for the large crystal it seems then most reasonable to attribute these differences in R value to differences in the quality of the mosaicity in the crystal, as the experimental conditions for all the experiments were identical. From the γ -ray rocking curves shown in Fig. 5 we know that the large crystal, rather than having a homogeneous distribu-

tion of dislocations, consists of misaligned regions of varying size, each representing a mosaic crystal in itself. The large R values are therefore not surprising. When the data for the large crystal are refined with the anisotropic mosaic model there are only minor improvements in the R values. For the small crystal, however, where the mosaicity observed by γ -ray diffractometry is quite homogeneous and where we have tried to introduce a distribution model in agreement with observations, the anisotropic refinement leads to a good improvement in the R values, especially for the long wavelength where the corrections for extinction are comparable with those for the large crystal. From this comparison we conclude that the defect structure in the large crystal is so different from what is assumed in the mosaic model that the introduction of an anisotropic mosaic spread represents only a minor change in the model for the defect structure of the sample and has therefore no effect on the R value.

Data collection was carried out at two wavelengths for the small crystal mainly as a data collection control, and we do find that the extinction parameters are insensitive to the change in wavelength when η^* is fixed. Another reason for collecting data at two wavelengths was to follow the behaviour of the temperature factor as a function of wavelength, although it was not the intention of this study to make an accurate determination of this quantity. As we did not correct for thermal diffuse scattering and as the detector aperture was kept the same for all measurements, one would expect the contribution from this effect to be larger at the lower wavelength, thereby reducing the corresponding temperature factor (Cooper & Rouse, 1968). This effect is observed for the anisotropic refinements but in addition a large difference is found between the temperature factors for the isotropic and the anisotropic refinements for the small crystal at the long wavelength. This difference seems to be correlated with the extinction correction. Quite large differences in the extinction factor, E , are

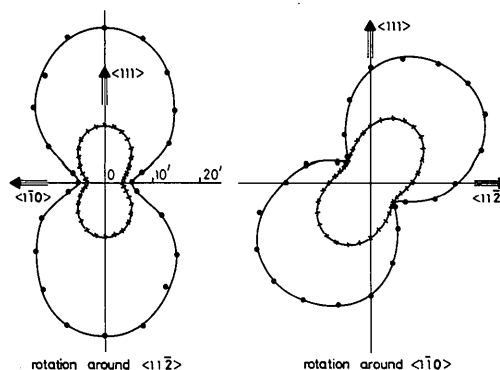


Fig. 8. Mosaic spread for the small crystal as a function of rotation about the scattering vectors $\langle 11\bar{2} \rangle$ and $\langle 1\bar{1}0 \rangle$ respectively: $\times - \times - \times$ cut through the mosaic distribution deduced from the crystal structure refinement. $\bullet - \bullet - \bullet$ results obtained by γ -ray diffractometry.

† Table 3 has been deposited with the British Library Lending Division as Supplementary Publication No. SUP 32563 (3 pp.). Copies may be obtained through The Executive Secretary, International Union of Crystallography, 13 White Friars, Chester CH1 1NZ, England.

observed when the two refinements are compared. For example for the series 0, 0, 1, $l=2,8$ the values of E are 0.64, 0.82, 0.90 and 0.94 for the isotropic refinement and 0.90, 0.95, 0.98 and 0.99 for the anisotropic refinement. This overcorrects some of the observed data at

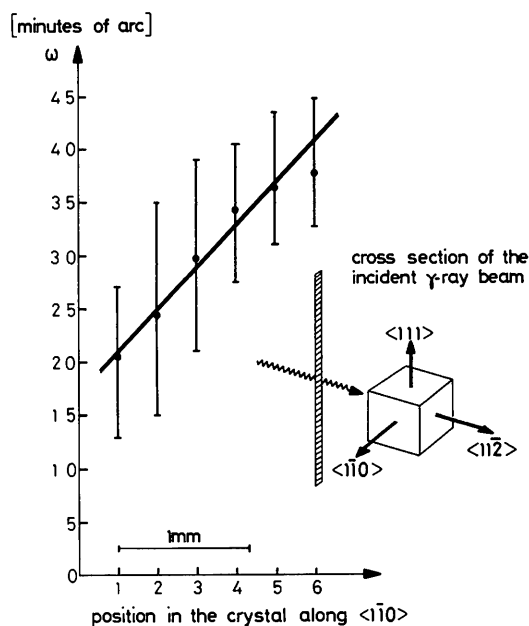


Fig. 9. Location of rocking curves indicated by the FWHH as a function of the measurement position in the crystal for a scan of the crystal along $1\bar{1}0$. The dots indicate the centre of gravity of the profile.

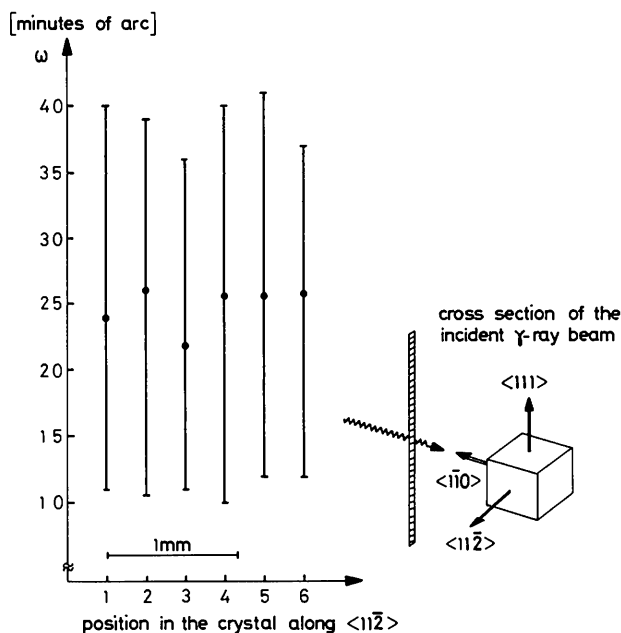


Fig. 10. Location of rocking curves as in Fig. 9. This time a scan of the crystal is made along $\langle 11\bar{2} \rangle$.

low angle, having as effect an increase in the scale factor and the temperature factor.

Comparing the relative scale factors k_x for the large and the small crystals at the short wavelength where the experimental geometry was identical, we find good agreement between the ratio of the scale factors obtained from anisotropic extinction refinement, $k_{\text{large}}/k_{\text{small}} = 1.830$, and the ratio of the scale factors deduced from counting times and crystal masses, $k_{\text{large}}/k_{\text{small}} = 1.810$, *i.e.* a difference of 1.1%.

Temperature factors did not alter excessively between the various anisotropic refinements, but the mean value of $u = 0.0064(2) \text{ \AA}^2$ is appreciably smaller than values obtained from X and γ -ray measurements (Battermann, Chipman & DeMarco, 1961; Jennings, Chipman & DeMarco, 1964; Hosoya & Yamagishi, 1966; Temkin, Henrich & Raccach, 1972; Freund, 1973, 1975a; Schneider, 1976), where the mean value is $0.0072(3) \text{ \AA}^2$. This clearly indicates the need for corrections for thermal diffuse scattering. On the other hand, we do not find any large disagreement among the results from the two crystals and so we can conclude that in this case the quality of the mosaic model has only little influence on the thermal parameters.

Various cuts through the observable mosaic distribution deduced from the crystal structure refinement using expression (2) for the small sample are given in Figs. 7 and 8 together with the corresponding results obtained by means of γ -ray diffractometry. The quantity given is the full width at half height (FWHH). There is very good agreement between neutron and γ -ray results for the smallest diameter of the peanut-shell-shaped mosaic distribution, but for the largest diameter of the peanut shell there is a large discrepancy. Some of the γ -ray rocking curves, especially the broader ones, have indications of a double peaked shape, which can indicate that the lattice planes are bent; this possibility can be checked easily by means of γ -ray diffractometry.

If, for example, we consider the case where the $\langle 111 \rangle$ direction is parallel to the ω axis of the γ -instrument, a series of rocking curves for the $2\bar{2}0$ reflexion can be measured in neighbouring volume elements of the sample by suitable choice of beam cross section and crystal position. Fig. 9 shows the FWHH of the rocking curves obtained as the sample was studied in a series of sections orthogonal to $\langle 1\bar{1}0 \rangle$. The FWHH is of the order of $15'$ and does not vary much. The centre of mass of the profile, however, changes its position on the ω scale proportional to the displacement of the sample and this indicates a bending of the lattice planes of $\sim 7'$ per mm, *i.e.* a total of $14'$ in the crystal. After a rotation of the sample of 90° around ω , rocking curves for the $22\bar{4}$ reflexion were measured in a similar manner. There the FWHH, shown in Fig. 10, is of the order of $30'$. The centre of mass oscillates in an angular range small compared to the FWHH, making it impossible to outline a continuous bend of the lattice planes. Measurements of

the same type were performed on the γ -diffractometer with the $\langle 1\bar{1}0 \rangle$ and the $\langle 11\bar{2} \rangle$ directions parallel to the ω axis and the results are summarized in Fig. 11, which shows an unfolded cube representing a model of the crystal. Each surface is characterized by $\langle hkl \rangle$ normal to the face. The results shown in Figs. 9 and 10 are indicated on the surfaces of the cube characterized by $\langle 111 \rangle$ and $\langle \bar{1}\bar{1}\bar{1} \rangle$. Along the $\langle 11\bar{2} \rangle$ direction we found no bending and the result is represented by a straight dashed band orthogonal to the crystal sections studied and with a width proportional to the FWHH of $\sim 30'$ of the rocking curves. From scanning along $\langle 1\bar{1}0 \rangle$ we deduced a curvature of the lattice planes represented in Fig. 11 by the dark curved band again orthogonal to the individual sections and with a width proportional to the FWHH of the rocking curves. In general in Fig. 11 bands are dashed in all cases where the angle describing the curvature was significantly smaller than the FWHH of the rocking curves or where the centre of mass oscillated irregularly. Fig. 11 shows qualitatively that the local mosaic structure is indeed superimposed on a macroscopic curvature of the lattice planes. For example, for the surface $\langle 111 \rangle$ in Fig. 11 the intrinsic mosaic spread and the curvature of the lattice planes determined from rocking curves measured at the $2\bar{2}0$ reflexion add together linearly to the overall mosaic spread measured at the $22\bar{4}$ reflexion. This relation also holds for the two other directions $\langle 1\bar{1}0 \rangle$ and $\langle 11\bar{2} \rangle$. On the basis of these experimental results we can now give a possible explanation for the observed peanut-shell-shaped mosaic distribution and the agreements and disagreements between neutron and γ -ray results. Let us first consider a plane parallel plate of a perfect copper crystal bent cylindrically with the large surface parallel to the (111) lattice planes. If one measures rocking curves at the 111 reflexion in transmission for azimuthal angles varying between $\psi = 0$ and 180° one finds two extreme values for the FWHH: the largest value dominated by the overall curvature of the lattice planes and the smallest value being very close to the FWHH of the diffraction profile for a perfect crystal, which in practice in γ -ray diffractometry is equal to the angular resolution of the instrument. If we assume the crystal to have a homogeneous mosaic structure then the smallest FWHH is governed by the intrinsic mosaic spread, whereas the largest value is the sum of the broadening due to the curvature and the local mosaic spread. A plot of the FWHH as a function of the azimuthal angle ψ will then give a shape similar to a section through a peanut shell as actually is observed in the small copper crystal.

As a result of these qualitative arguments the smallest diameters of the peanut-shell shaped mosaic distribution shown in Figs. 7 and 8 are unaffected by the macroscopic bending of the lattice planes and therefore the mosaic spread parameters obtained from the structure refinement of the neutron data of the small crystal will be equal to the results obtained from γ -ray dif-

fractometry, and good agreement is observed. For the azimuthal angles ψ corresponding to the large diameters of the peanut shell it is plausible that the FWHH of the γ -ray rocking curves are larger than the mosaic spread parameters from the structure refinement as the extinction will mainly be governed by the intrinsic mosaic spread. A more precise discussion is difficult for two reasons: First it is difficult to determine precisely the actual bending of the lattice planes in the crystal by means of γ -ray diffractometry and second the extinction theories applied in structure refinements do in principle not apply to this crystal with bent planes because the coupling constant $\sigma(\omega, r)$ is now also a function of position in the crystal.

The macroscopic curvature of the lattice planes observed by γ -ray diffractometry in the small crystal is probably due to the fact that for technical reasons the crystal was deformed by pressing and not by pulling, the last being in principle the better technique to obtain a homogeneous arrangement of dislocations. Recently further progress has been made in plastic deformation of large nearly perfect single crystals (Freund, 1976), so that samples of copper, silicon and germanium single crystals of homogeneous defect structure and various mosaic spread can be produced in a routine way. As shown by Hohlwein (1975), it is easy to bend copper single crystals cylindrically up to a radius of curvature of the order of 1 m without disturbing the homogeneity of the mosaic structure in the sample. It would be interesting to develop an extinction theory for such a crystal where $\sigma(\omega, r)$ could be described analytically. A comparison of the extinction parameters from structure refinements of neutron data measured at various wavelengths with the results obtained by means of γ -ray diffractometry would represent a sensitive test of this further-developed extinction theory. As a bent mosaic crystal represents one of the simplest cases of a position-

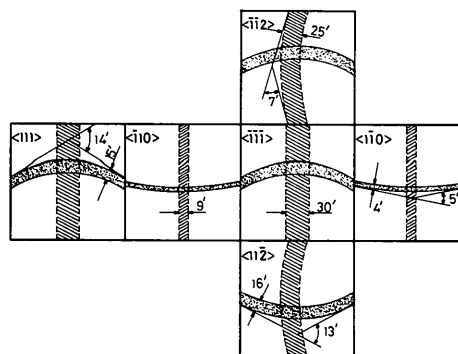


Fig. 11. Representation of the crystal cube. The cube is unfolded and the faces are indicated by $\langle hkl \rangle$. For a given $\langle hkl \rangle$ parallel to the ω axis of the γ -diffractometer the width of a band on the face $\langle hkl \rangle$ is proportional to the mosaic width in a crystal section orthogonal to the band. Crystal curvature is indicated by the lines being curved.

dependent mosaic structure, such a theory could provide a much better understanding of the consequences of inhomogeneities in the sample defect structure for the reliability of the crystal parameters obtained from structure refinement. This is important because probably for most of the imperfect single crystals used in crystallographic measurement the simple mosaic model is not a physically adequate description of the defect structure.

Conclusions

A distribution of dislocations can be created in copper, silicon and germanium single crystals by plastic deformation such that the mosaic model represents well this type of defect structure, and therefore these samples are well suited to a systematic study of extinction effects. As a result of the availability at the Institut Laue-Langevin of very short neutron wavelengths of the order of 0.5 Å, a rather large number of independent reflexions can be measured even for these simple compounds, so that normal structure refinements work well. Combining γ -ray measurements and neutron diffraction studies on single copper crystals allowed us to carry out comparisons between mosaic distributions as observed from γ -ray rocking curves and neutron diffraction refinements.

In order not to do make any comparisons among the various theories of extinction, we chose crystals which only needed rather small corrections, not exceeding 30%, but to get good agreement at first we had to go to anisotropic extinction models; only after the γ -ray measurements had been well understood could we introduce a physically reasonable model for the anisotropy. We would therefore like to suggest that mosaic distribution curves are used as a guide for anisotropic refinement models. These can indeed be obtained by a simple correction for the beam divergence from the diffraction experiment, as was done with some profiles obtained on the neutron diffractometer, with the assumption that the rocking curves are reasonably well shaped, and provided the mosaic distribution width is similar to the instrumental width. Finally we would like to suggest that these types of compounds with well-defined mosaic distribution as well as well-defined curvatures should be used to develop further extinction theories, as for these crystals defect patterns similar to but simpler than the general real case are available.

We are indebted to Dr A. Freund for supplying us with the samples used in this study and for critical reading of the manuscript.

Note: At the stage of publication it was pointed out to us by Dr R. J. Nelmes that the non-ellipsoidal behaviour of the observable mosaic distribution is a normal feature of the observable distribution in the formalism of Thornley & Nelmes (1974). This formalism is based on a function $P_2(\Delta, \mathbf{D})$ which describes

the probability of a mosaic block having a misorientation about any direction of such a magnitude that it has a component Δ about \mathbf{D} , and this is the adequate description of an ω scan for measurement of the integrated intensity where all mosaic blocks pass through the Bragg position. Normally this is assured by the vertical divergence of the incident beam and a sufficiently large detector aperture. As a result of the Thornley-Nelmes theory the observable mosaic distribution is a fourth-order surface when the mosaic distribution is ellipsoidal and the variation of η with \mathbf{D} will be very similar to the one introduced in (2). Although the Coppens-Hamilton (1970) formalism includes in the probability function $P_1(\Delta, \mathbf{D})$ only those mosaic blocks having a misorientation Δ about \mathbf{D} , the difference between the results of the two models is generally assumed to be small for weak extinction.

New refinements of the data for the small crystal now using the Thornley-Nelmes formalism gave results which were in very good agreement with the results obtained by means of the modified Coppens-Hamilton expression for all parameters as well as for the derived observable mosaic distribution. For the three orthogonal sections shown in Figs. 7 and 8 the maximum differences between the mosaic width for the two models were at most 1' corresponding to one estimated standard deviation, and the R indices are identical. Our conclusion would therefore be in the present case that the anisotropy is so strong that it is beyond the limit where the Coppens-Hamilton formalism works, and is not necessarily due to the curvature of the lattice planes as we have assumed before. However, we are left with the question of how the space dependence of the coupling constant $\sigma(\omega, \mathbf{r})$ affects the diffraction process.

References

- BATTERMAN, B. W., CHIPMAN, D. R. & DEMARCO, J. J. (1961). *Phys. Rev.* **122**, 68-74.
- BECKER, P. J. & COPPENS, P. (1974a). *Acta Cryst.* **A30**, 129-147.
- BECKER, P. J. & COPPENS, P. (1974b). *Acta Cryst.* **A30**, 148-153.
- BECKER, P. J. & COPPENS, P. (1975). *Acta Cryst.* **A31**, 417-425.
- BONNET, M., DELAPALME, A., BECKER, P. & FUESS, H. (1976). *Acta Cryst.* **A32**, 945-953.
- COOPER, M. J. & ROUSE, K. D. (1968). *Acta Cryst.* **A24**, 405-410.
- COOPER, M. J. & ROUSE, K. D. (1970). *Acta Cryst.* **A26**, 214-223.
- COOPER, M. J. & ROUSE, K. D. (1976). *Acta Cryst.* **A32**, 806-812.
- COPPENS, P. (1975). Program *LINEX*. Chemistry Department, State University of New York at Buffalo, Acheson Hall, Buffalo, NY 14214, USA.
- COPPENS, P. & HAMILTON, W. C. (1970). *Acta Cryst.* **A26**, 71-83.
- DARWIN, C. G. (1914). *Phil. Mag.* **27**, 315, 657.
- DARWIN, C. G. (1922). *Phil. Mag.* **43**, 800.

- FREUND, A. (1973). PhD Thesis, Technische Universität München.
- FREUND, A. (1975a). *Anomalous Scattering*, Edited by S. RAMASESHAN & S. C. ABRAHAMS, pp. 69–84. Copenhagen: Munksgaard.
- FREUND, A. (1975b). *Nucl. Instrum. Meth.* **124**, 93–99.
- FREUND, A. (1976). *Progress in Neutron Monochromator Development at the Institut Laue-Langevin*. Proceedings of the Gatlinburg Conference, June 1976, USA.
- FREUND, A. & SCHNEIDER, J. R. (1972). *J. Cryst. Growth*, **13/14**, 247–251.
- HOHLWEIN, D. (1975). *J. Appl. Cryst.* **8**, 465–468.
- HOSOYA, S. & YAMAGISHI, T. (1966). *J. Phys. Soc. Japan*, **21**, 2638–2644.
- JENNINGS, L. D., CHIPMAN, D. R. & DEMARCO, J. J. (1964). *Phys. Rev.* **135**, 1612–1615.
- LARSON, A. C. (1967). *Acta Cryst.* **23**, 664.
- LEHMANN, M. S. & LARSEN, F. K. (1974). *Acta Cryst.* **A30**, 580–584.
- Neutron Cross Sections* (1955). BNL Report 325, Brookhaven National Laboratory, Upton, NY 11973, USA.
- SCHNEIDER, J. R. (1974a). *J. Appl. Cryst.* **7**, 541–546.
- SCHNEIDER, J. R. (1974b). *J. Appl. Cryst.* **7**, 547–554.
- SCHNEIDER, J. R. (1975a). *J. Appl. Cryst.* **8**, 195–201.
- SCHNEIDER, J. R. (1975b). *J. Appl. Cryst.* **8**, 530–534.
- SCHNEIDER, J. R. (1976). *J. Appl. Cryst.* **9**, 394–402.
- SCHNEIDER, J. R. (1977). *Acta Cryst.* **A33**, 235–243.
- SEGER, A. A. (1965). Editor, *Moderne Probleme der Metallphysik*. Vol. 1. Heidelberg: Springer Verlag.
- TEMKIN, R. J., HENRICH, V. E. & RACCAH, P. M. (1972). *Phys. Rev.* **B6**, 3572–3581.
- THORNLEY, F. R. & NELMES, R. J. (1976). *Acta Cryst.* **A30**, 748–757.
- ZACHARIASEN, W. H. (1967). *Acta Cryst.* **23**, 558–564.

Acta Cryst. (1977). **A33**, 800–804

A Structure-Factor Least-Squares Refinement Procedure for Macromolecular Structures using Constrained and Restrained Parameters

BY JOEL L. SUSSMAN,* STEPHEN R. HOLBROOK, GEORGE M. CHURCH AND SUNG-HOU KIM

Department of Biochemistry, Duke University Medical Center, Durham, North Carolina 27710, USA

(Received 22 February 1977; accepted 18 April 1977)

A method of structure-factor least-squares refinement of *constrained* groups linked by distance *restraints* has been developed for the refinement of macromolecular structures. Each constrained group can have any number of variable dihedral rotation parameters within the group in addition to the rigid-body translational, rotational and thermal parameters. The matrix of normal equations may be either full or sparse and provision is made for solution by matrix inversion or the conjugate-gradient iterative method. This procedure has been successfully used for 3 Å data and should be applicable even for lower-resolution data and especially for cases with a poorer data-per-atom ratio. The structure of yeast phenylalanine tRNA has been refined with this procedure from a starting crystallographic *R* value of 42% to a final *R* value of 25% with isotropic 'group' thermal parameters and 22% with isotropic atomic thermal parameters for 8207 independent reflections at 2.7 Å resolution. The proper stereochemistry of bond distances, angles and van der Waals contacts for the restrained atoms was maintained within reasonable limits throughout the refinement. Although originally developed for nucleic acids, this procedure is directly applicable to the refinement of protein structures. In addition, a combination of applying distance restraints between groups and least-squares fitting of these groups to target coordinates has been used purely as an idealization process for imposing proper stereochemistry on an approximate model.

Introduction

As the number of macromolecules for which an approximate model has been derived by X-ray diffraction methods has increased, several methods of structure refinement have been tried.

To refine protein structures in *real space*, Freer, Alden, Carter & Kraut (1975) automated the difference Fourier technique of obtaining shifts, and introduced differential methods of calculating the slope of the electron density at the grid points in conjunction with imposition of restraints between cycles. Diamond

(1971) has devised a procedure for minimizing the difference between an electron density map and a model density map, calculated assuming a Gaussian distribution of electron densities centered at the atomic positions from the current model, by changing only torsional angles and some bond angles of the constrained model. Among others, Deisenhofer & Steigemann (1975) applied this procedure together with Fourier maps calculated with new phases after each cycle to refine the structure of the pancreatic trypsin inhibitor.

The structure refinement of macromolecules in *reciprocal space* was pioneered by Watenpaugh, Sieker, Herriot & Jensen (1973), who showed that it was possible to refine a protein structure by a least-squares

* Present address: Department of Structural Chemistry, The Weizmann Institute of Science, Rehovot, Israel.